

Structure of Poly(vinyl alcohol) Gels Studied by Wide- and Small-Angle Neutron Scattering

T. Kanaya,* M. Ohkura, and K. Kaji

Institute for Chemical Research, Kyoto University, Uji, Kyoto-fu 611, Japan

M. Furusaka and M. Misawa†

*National Laboratory for High Energy Physics, Tsukuba, Ibaraki-ken 305, Japan**Received February 23, 1994; Revised Manuscript Received June 27, 1994**

ABSTRACT: The structure of poly(vinyl alcohol) (PVA) gels formed in a mixture of deuterated dimethyl sulfoxide (DMSO- d_6) and heavy water at 23 °C has been investigated by wide- and small-angle neutron scattering techniques. It was directly confirmed from the wide-angle neutron scattering measurements that cross-linking points or junction points in the gels are crystallites. In the small-angle scattering measurements, it was found that the scattering intensity $I(Q)$ decreases with Q according to the -4th power law (Porod's law) in the Q range above 0.05 \AA^{-1} where $Q = 4\pi \sin \theta / \lambda$ (2θ and λ are scattering angle and wavelength of neutron, respectively), suggesting that the surface of the crystallites has a clear boundary. On the other hand, the Q dependence of the scattering intensity $I(Q)$ can be described by $I(0)/[1 + \xi^2 Q^2]$ in the Q range below 0.035 \AA^{-1} , where ξ is a correlation length. The correlation length ξ was assigned to the average distance between the neighboring crystallites. Distance distribution function $P(r)$ which is defined by inverse Fourier transformation of scattering intensity $I(Q)$ was also calculated in order to see another aspect of the scattering intensity. Two peaks or shoulders at about 70 and 200 Å were recognized in the calculated $P(r)$. The former and the latter have been attributed to the intra- and intercrystallite correlations, respectively. By separating the two correlations, the distribution of the crystallites is discussed.

Introduction

It is well-known that solutions of poly(vinyl alcohol) (PVA) show a transition from sol to gel on cooling in various solvents.¹⁻⁹ Recently, it was reported^{2,3} that PVA gels formed from solutions of mixtures of dimethyl sulfoxide (DMSO) and water show very interesting features; e.g., the gels obtained below 0 °C are transparent, the elasticity is very high, and the gelation rate is very fast compared with those from aqueous solutions.^{3,4} These properties depend on the ratio of DMSO to water. In the previous paper,³ we determined the sol-gel diagram and observed the turbidity of the PVA gels in a mixture of DMSO and water (60/40, v/v) as functions of temperature and PVA concentration. It was pointed out that the gelation from the mixture occurs without phase separation below -20 °C, while the phase separation plays a very important role for the gelation above -20 °C. However, the structure of the gels is not well understood from microscopic viewpoints.

With regard to PVA in ethylene glycol-water mixtures, Pines and Prins⁵ reported that PVA gels were formed via liquid-liquid phase separation or spinodal decomposition followed by the crystallization of PVA chains. The spinodal decomposition in aqueous PVA solutions has been detected using light scattering techniques by Komatsu et al.⁶ Small-angle neutron scattering (SANS) measurements have been extensively performed on aqueous PVA gels with and without borate ions by Wu et al.^{7,8} and Shibayama et al.⁹ The wavelength range accessible by SANS is usually shorter than light scattering (LS) so that it is difficult for the former to detect the network structure of polymer molecules in a gel cluster. In their studies, they focused on the change of local concentration fluctuation by gelation in terms of correlation length ξ .

As for the gelation from homogeneous solution, the length scale of the fluctuations or the correlation length

ξ is the size of an individual polymer coil at around the critical concentration C^* where the polymer chains start to overlap. The correlation length should increase near C^* or slightly above C^* when neighboring chains are cross-linked because the molecular weight increases by cross-linking. On the other hand, in the solutions with concentrations much higher than C^* , it is expected that the local concentration fluctuation is not significantly affected by gelation or formation of cross-linking points because the number of neighboring chains around a given chain is large and all the chains are highly interpenetrated. It is noted that this picture can be applied only to systems where gelation occurs from homogeneous solutions without liquid-liquid phase separation and cross-linking points are not crystallites. If crystallites are formed in gels, significant concentration fluctuations would be governed by a distribution of the crystallites because the crystallite-crystallite correlation is much stronger than the other correlations such as segment-segment correlation.

In this work, we have first investigated the structure of PVA gels formed in a mixture of DMSO- d_6 and D_2O (60/40, v/v) at 23 °C using a wide-angle neutron scattering (WANS) technique in order to confirm the cross-linking points are crystallites, and then small-angle neutron scattering (SANS) measurements have been conducted to see the gel structure on a larger spatial scale. As pointed out in the previous paper,³ above -20 °C liquid-liquid phase separation takes place in the DMSO/water solution followed by gelation, and as will be shown later, the cross-linking points of the gel are crystallites. In such systems, the local concentration fluctuation is no more governed by the PVA chain coil size even at C^* . Therefore, we will discuss the SANS results in terms of the size and the distribution of the crystallites.

Experimental Section

Materials. Fully saponified atactic poly(vinyl alcohols) (at-PVA) with number-average degrees of polymerization $P_n = 1640$, 590, and 186 were used for the small-angle neutron scattering measurements. The molecular weight distributions, M_w/M_n , are

* Present address: Faculty of Science, Niigata University, Niigata 950-21, Japan.

† Abstract published in *Advance ACS Abstracts*, August 15, 1994.

1.97, 1.61, and 2.04 for $P_n = 1640, 590$, and 186, respectively. The details of the characterization of the PVA's were reported in the previous paper.³ Deuterated atactic poly(vinyl alcohol) (at-PVA- d_4) was employed for the wide-angle neutron scattering measurements. The number-average degree of polymerization is 1700, and the M_w/M_n is 2.01, which was supplied by Kuraray Co., Ltd. The solvent used for both the wide- and small-angle neutron scattering was a mixture of deuterated dimethyl sulfoxide (DMSO- d_6) and heavy water (D_2O) with a ratio of 60/40 by volume.

Gel samples were prepared as follows. A given amount of PVA was dissolved in the solvent at about 130 °C to be homogenized in a sealed glass tube in vacuum in order to avoid contamination from H_2O in the atmosphere. After the homogenization, the solution was transferred to a quartz scattering sample cell, quickly quenched in a bath kept at 23 °C, and allowed to stand for the PVA sample for 1 day (24 h) for SANS measurements and for the PVA- d_4 sample for 3 days and 20 days for the WANS measurements. Here it should be noted that the gelation rate of PVA- d_4 , which is a sample for WANS measurements, is about 3 times slower than hydrogenated PVA. Times required for gelation are 60 and 190 min for the PVA and PVA- d_4 solutions with a polymer concentration of 10 g/dL, respectively. The standing time of 3 days for the PVA- d_4 solution, which is 3 times longer than that for the PVA solution, is due to this reason. We carried out SANS measurements on the PVA- d_4 gel 3 days after quenching to confirm that the gel state is identical with that of the PVA gel 1 day (24 h) after quenching and found that the scattering profiles are essentially the same within experimental error while the scattering intensity of the PVA- d_4 gel is very weak due to the low scattering contrast.

Measurements. SANS measurements were performed with the SAN spectrometer¹⁰ at the National Laboratory for High Energy Physics (KEK), Tsukuba, Japan. This spectrometer is a time-of-flight (TOF) type of small-angle scattering machine and sits at the exit of a neutron guide tube C1 which views a solid methane moderator at 20 K. A converging Soller slit is used before a sample, which enables us to use larger samples (20 mm in width and 30 mm in height). The sample position is 19 m from the moderator, and a two-dimensional area detector was fixed at a position of 3 m from the sample in a vacuum scattering chamber. The Q ranges covered with this detector for neutron wavelengths from 3 to 11 Å is $0.008 < Q < 0.2 \text{ Å}^{-1}$. The resolution of the spectrometer $\Delta Q/Q$ is less than 10% even at the lowest Q value. The sample cell is made of quartz 1 mm thick, and the inner size of the cell is 20 mm wide, 30 mm high, and 2 mm thick. The observed scattering intensities were corrected for the incident neutron spectrum, detector efficiency, sample transmission, and background scattering. The incoherent scattering contribution from hydrogen atoms of the gel samples was evaluated by measuring the scattering intensity from hydrogenated methanol dissolved in the deuterated mixture of DMSO- d_6 and D_2O solvent so that the hydrogen concentration would be the same as that of a given gel sample. The sample temperature was controlled at $23 \pm 0.5 \text{ °C}$ during the measurements.

It is emphasized that the Q range covered with the SANS machine used here¹⁰ is extended to a rather high Q range than those of the usual SANS machines at reactors. Therefore, we can access the so-called Porod region in the present measurements, which is a special advantage for studies of gels with cross-linking points of crystallites.

WANS measurements were carried out with a high-intensity total scattering spectrometer of TOF type, HIT,¹¹ installed at the pulsed thermal neutron source (H_2O moderator at ambient temperature) in the National Laboratory for High Energy Physics, Tsukuba, Japan. This spectrometer has seven detector banks at average scattering angles of 8.1, 13.8, 23.5, 30.1, 42.9, 91.3, and 149.6°, which can cover a very wide Q range from 0.5 to 50 Å^{-1} using neutron wavelengths of 0.3–4 Å. The cylindrical sample cell 50 mm high and 8 mm in inner diameter is made of a zero scattering alloy of Ti/Zr with thickness 0.1 mm. The Q resolution has been evaluated by a Monte Carlo method for each scattering angle.¹¹ The observed neutron scattering intensity was corrected for attenuation due to both the sample and cell, subtraction of scattering intensity from the cell, the incident neutron spectrum, and the neutron emission delay time.¹¹

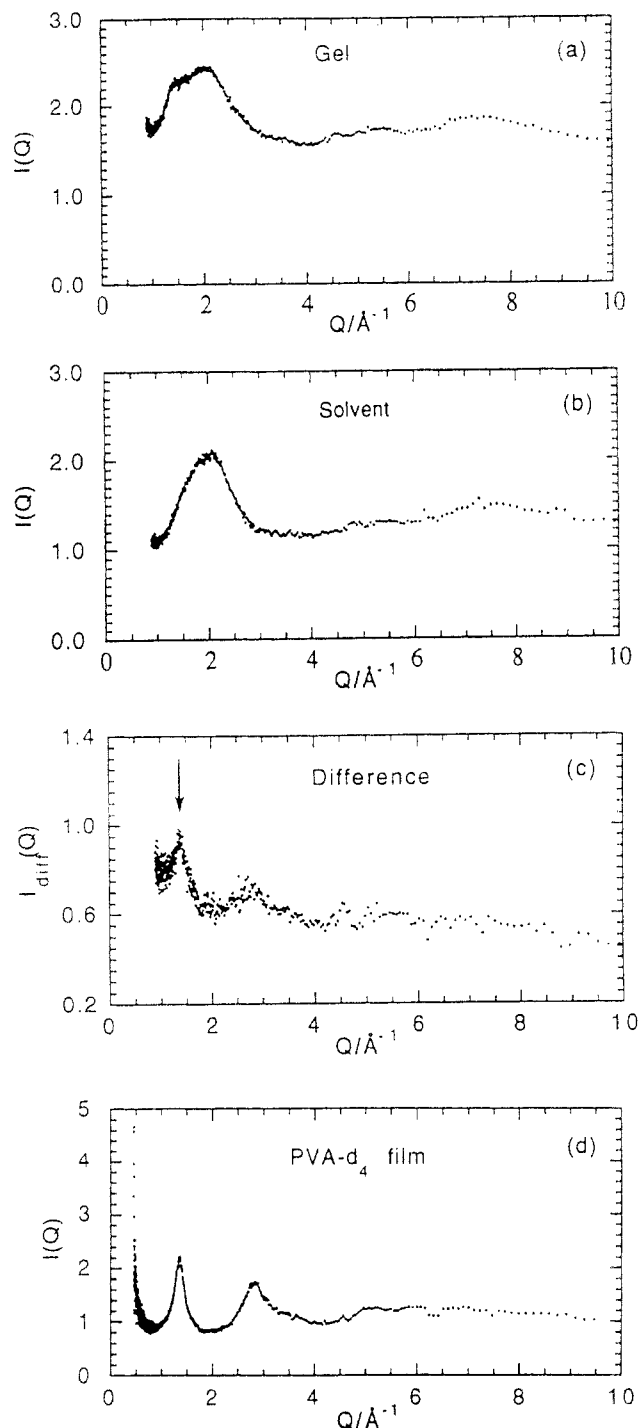


Figure 1. Wide-angle neutron scattering intensity $I(Q)$ measured by the HIT spectrometer. (a) PVA- d_4 gel in DMSO- d_6/D_2O (60/40, v/v) with $C_p = 10 \text{ g/dL}$. (b) Solvent [DMSO- d_6/D_2O (60/40, v/v)]. (c) Difference scattering intensity $I_{\text{diff}}(Q)$ between the PVA- d_4 gel and the solvent. The subtraction was made by taking into account the solvent molecules replaced by PVA- d_4 in the gel. (d) PVA- d_4 solid film. The degree of crystallinity is about 45%.

Results and Discussion

Wide-Angle Neutron Scattering. PVA is one of the typical crystalline polymers, so that cross-linking points or junction points in the gels are believed to be crystallites though it has never been directly confirmed. First of all, we conducted WANS measurements of at-PVA- d_4 gel at a PVA concentration of 10 g/dL in a mixture of DMSO- d_6 and D_2O (60/40, v/v), which was obtained 20 days after quenching to 23 °C from the homogeneous solution at 130 °C. The observed scattering intensities $I(Q)$'s are shown for the gel and the solvent in parts a and b of Figure 1, respectively, in the Q range of 0.8–10 Å^{-1} . These two scattering curves are very similar to each other especially

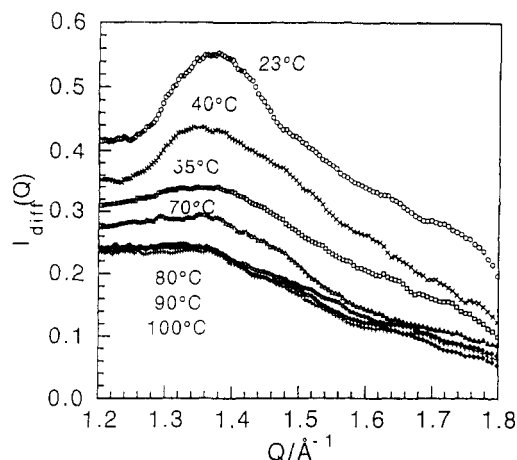


Figure 2. Wide-angle neutron scattering intensities $I(Q)$ of PVA- d_4 gel as a function of temperature. Scattering intensity from the mixed solvent of DMSO- d_6 and D_2O (60/40, v/v) at the corresponding temperature has been subtracted.

in the Q range above 2.0 \AA^{-1} , while we can clearly recognize a weak shoulder at about $Q = 1.40 \text{ \AA}^{-1}$ in the scattering curve of the gel, but it is absent in that of the solvent. When the scattering intensity of the solvent is subtracted from that of the gel after correcting for the volume of solvent molecules replaced by PVA molecules, Figure 1c is obtained. The error in the difference spectra is about 10%. Here the strongest peak is observed at $Q = 1.39 \text{ \AA}^{-1}$ which corresponds to the overlapping Bragg diffractions from (101) and (10 $\bar{1}$) planes of PVA crystals.¹² For comparison, the scattering curve from a PVA- d_4 solid film measured by the HIT spectrometer is also shown in Figure 1d. The difference scattering curve between the gel and the solvent (Figure 1c) is basically identical with that of the solid film though the widths of the peaks in the difference scattering curve are rather broader than those of the film. This may be due to the small crystallites in the gel. It has therefore been confirmed that there exist crystallites in the PVA gel though it is not proved at this stage whether or not they are the cross-linking points in the PVA gel.

In order to confirm that the crystallites are the cross-linking points, WANS measurements were conducted as a function of temperature, focusing the strongest overlapping Bragg peaks at $Q = 1.39 \text{ \AA}^{-1}$. The PVA- d_4 gel with a polymer concentration of 10 g/dL was used for the measurements 3 days after quenching to 23 °C from the homogeneous solution at 130 °C. Note that the Bragg peaks are slightly broader than those of the PVA- d_4 gels obtained 20 days after quenching. It is probably due to an aging effect. The temperature dependence of the scattering intensity $I(Q)$ from the gel is shown in Figure 2 where the scattering intensity from the solvent at the corresponding temperature was subtracted. The Bragg peaks at $Q = 1.39 \text{ \AA}^{-1}$ are clearly observed at 23 °C. The intensity gradually decreases with increasing temperature and the Bragg peaks are no longer observed in the scattering curve above 80 °C. The scattering intensity at $Q = 1.39 \text{ \AA}^{-1}$ is plotted against temperature in Figure 3. The intensity decreases approximately linearly with increasing temperature and becomes independent of temperature above about 75 °C. This temperature agrees well with the melting temperature T_m of the PVA gel determined by macroscopic observation.³ This result strongly suggests that the cross-linking points of the gel are crystallites.

The scattering intensity at off-Bragg positions also decreases with increasing temperature, the decrease of which is too large to be explained by a temperature factor. The off-Bragg intensity at $Q = 1.22 \text{ \AA}^{-1}$ is plotted as a

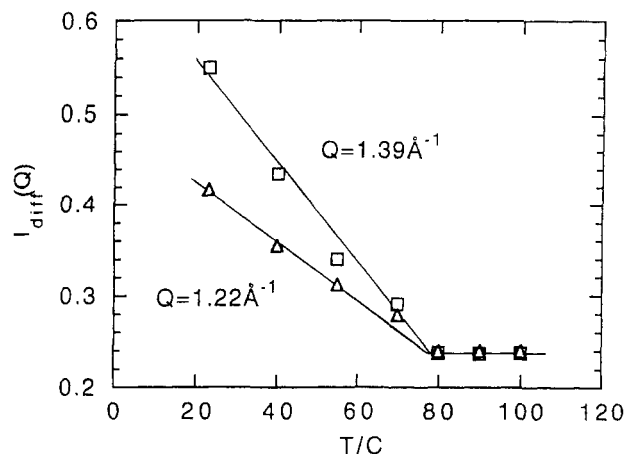


Figure 3. Temperature dependencies of the scattering intensities at the Bragg peak position ($Q = 1.39 \text{ \AA}^{-1}$) and the off-Bragg position ($Q = 1.22 \text{ \AA}^{-1}$) near the Bragg peak. The temperature dependencies are almost identical, suggesting that the intensity at the off-Bragg position may be due to scattering from amorphous-like parts around the crystallites.

function of temperature also in Figure 3. The intensity indicates a temperature dependence similar to that of the overlapping Bragg peak intensity at $Q = 1.39 \text{ \AA}^{-1}$; it decreases with increasing temperature and becomes independent of temperature above about 75 °C. This fact suggests that amorphous-like structure of PVA exists near or around the crystallites, and it is dissolved in the solvent in accordance with the melting of the crystallites. The intensity at the off-Bragg position near the Bragg peak may be assigned to the amorphous parts of PVA in the gels, as is well-known in the bulk sample.

From the above experiment, we believe that it has been directly confirmed that the cross-linking points of the PVA gels in the mixed solvent of DMSO- d_6 and D_2O are crystallites. This gives us a basis for interpretation of the SANS data presented in the next section.

Small-Angle Neutron Scattering. SANS measurements were made on the PVA gels and sols in DMSO- d_6 / D_2O (60/40, v/v) at 23 °C as functions of PVA concentration and degree of polymerization. Figure 4 shows the scattering intensity $I(Q)$ of the PVA gels with a degree of polymerization of 1640 as a function of PVA concentration ranging from 0.5 to 10 g/dL, which is plotted in double-logarithmic form after normalizing by the PVA concentration C_p . In the Q range above 0.05 \AA^{-1} , the scattering intensity $I(Q)$ decreases with increasing Q according to the -4 th power law for all the concentrations.

$$I(Q) \sim Q^{-4 \pm 0.1} \quad (1)$$

This Q dependence corresponds to the so-called Porod's law, indicating that the surfaces of the crystallites in the PVA gels have a rather clear boundary. The PVA used here is atactic so that the crystallites are composed of a combination of tactic sequences of various lengths. This should give rise to surface roughness on the order of the size of the monomers, but it may be neglected within experimental error in the Q range where Porod's law was observed. The critical gelation concentration C_g^* of the PVA solution was 1.25 g/dL for $P_n = 1640$ at 23 °C.³ It means that the samples with the PVA concentrations $C_p = 0.5$ and 1.0 g/dL are not macroscopically gels but sols. Nevertheless, the fact that the scattering intensity of these samples showed the -4 th power law in the Q range above 0.05 \AA^{-1} suggests that there exist crystallites even in the sol states and their boundaries are rather clear. The gels and sols are opaque³ at 23 °C which was explained to be due to the liquid-liquid phase separation or spinodal

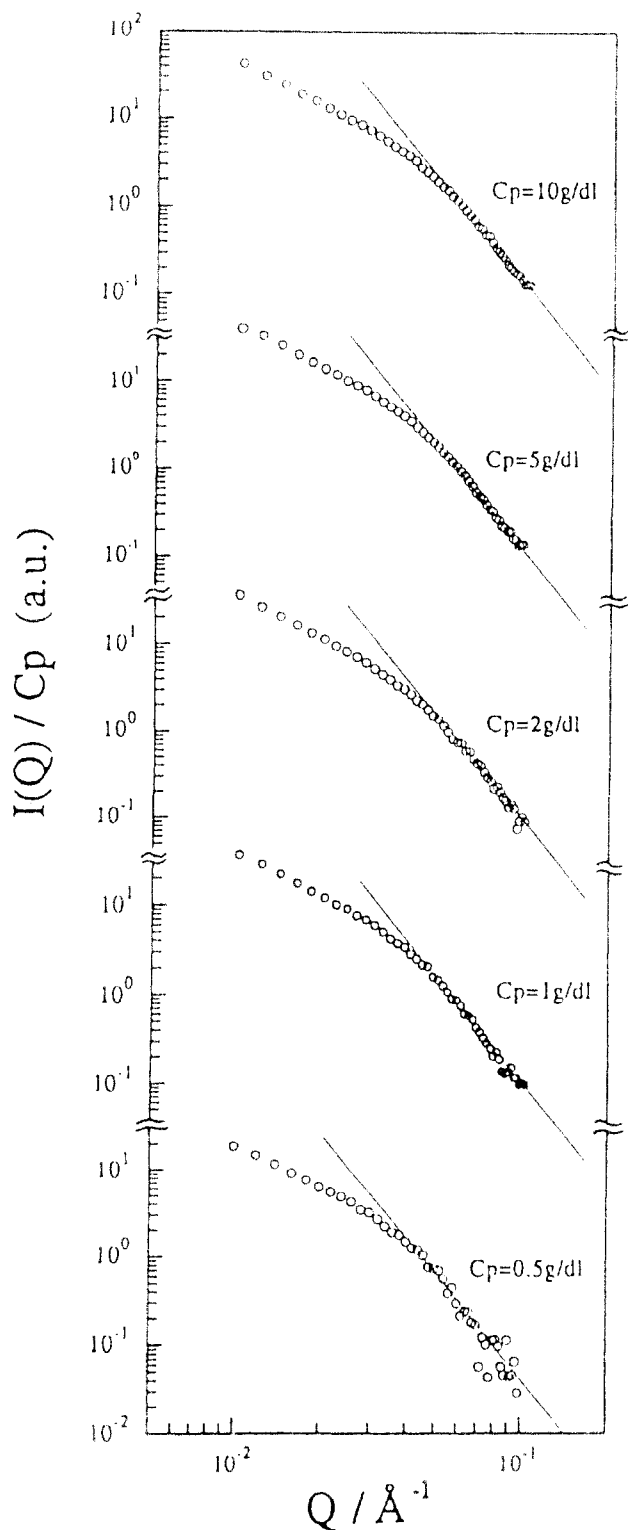


Figure 4. Small-angle neutron scattering intensity $I(Q)$ of PVA gels ($C_p = 10, 5$, and 2 g/dL) and sols ($C_p = 1.0$ and 0.5 g/dL) in $\text{DMSO-}d_6/\text{D}_2\text{O}$ (60/40, v/v) at 23°C . The intensity is normalized by C_p . The slope of the solid lines is -4 ± 0.1 .

decomposition of the system into concentrated and diluted phases before gelation.³ In this situation, gelation occurs in the concentrated phase, and the three-dimensionally connected network of this phase results in a macroscopic gel. Here it should be noted that the gelation occurs even below the overlap concentration, C^* , of PVA molecules if the concentration in the concentrated phase is larger than C^* . When the connection of the concentrated phase is not high enough to make an infinite three-dimensional network, gelation cannot occur macroscopically. Even in that case crystallization may take place in the concentrated phase. In other words, the PVA sol may have a "microgel"

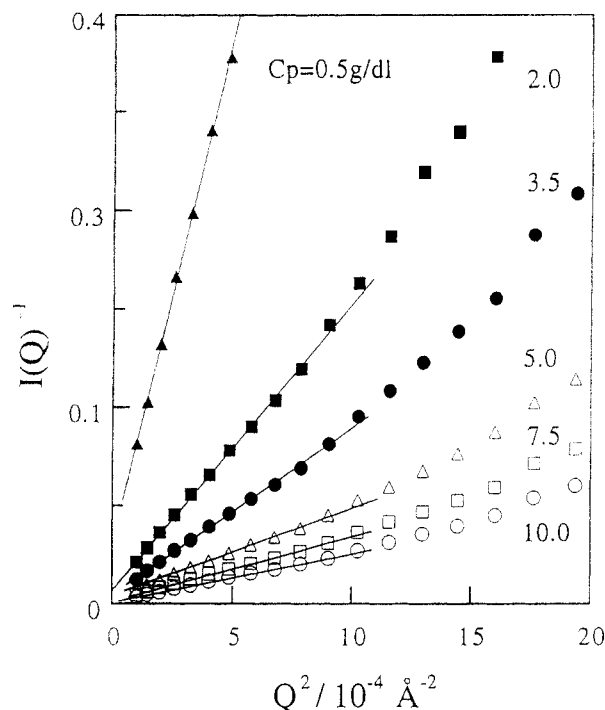


Figure 5. Inverse of small-angle scattering intensity $I(Q)^{-1}$ against Q^2 for various PVA concentrations in the Q range below ca. 0.045 \AA^{-1} . Correlation length ξ was evaluated from the straight lines in the figure. $P_n = 1640$.

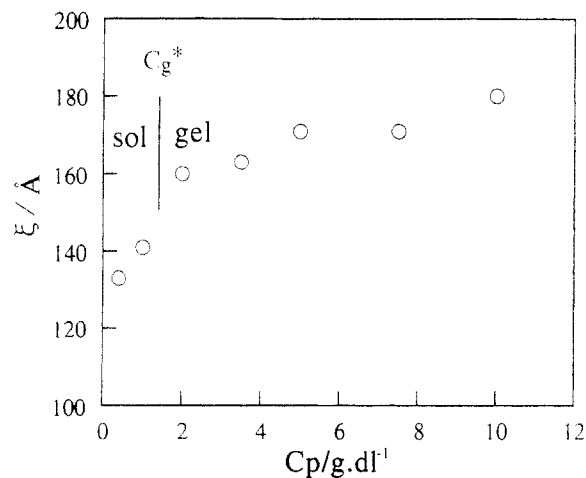


Figure 6. Correlation length ξ of PVA gels and sols in $\text{DMSO-}d_6/\text{D}_2\text{O}$ (60/40, v/v) for $P_n = 1640$ as a function of PVA concentration C_p . The critical gelation concentration C_g^* is 1.25 g/dL for $P_n = 1640$ at 23°C .

structure which is very similar to that of the macroscopic gels as far as it is observed in the Q range accessible in the present measurements.

The inverse of the scattering intensity $I(Q)^{-1}$ is plotted against Q^2 in the Q range below 0.045 \AA^{-1} in Figure 5. As seen in the figure, straight lines can be obtained for all the concentrations. It means that the Q dependence of $I(Q)$ in the Q range below ca. 0.035 \AA^{-1} can be described by the Ornstein-Zernike (OZ) formula

$$I(Q) = I(0)/(1 + \xi^2 Q^2) \quad (2)$$

where ξ is a correlation length and $I(0)$ is the scattering intensity at $Q = 0$. The concentration dependence of the correlation length ξ is shown in Figure 6 for PVA with $P_n = 1640$. Roughly speaking, the values of ξ in the gel states ($C_p > 1.25$ g/dL) are around 170 \AA and almost independent of the PVA concentration C_p . As the cross-linking points of the PVA gels are crystallites, the correlation length ξ can be related to the intercrystallite distance. This idea

is supported by the fact that the correlations between the crystallites are very strong compared with other correlations such as correlation between noncrystallized polymer chain segments. Further, the nearest-neighbor crystallite correlation may be the main contribution to ξ because the crystallites are considered to be located irregularly in the gels. The observation that ξ is almost independent of the concentration suggests that the cross-linking points are not homogeneously distributed in the whole system. As mentioned before, liquid-liquid phase separation or spinodal decomposition occurs in the DMSO/water (60/40, v/v) solution of PVA at 23 °C, and the solution is separated into concentrated and diluted phases before gelation. It is therefore considered that the infinite three-dimensionally connected network is formed in the concentrated phase where crystallization mainly occurs, leading to the inhomogeneous distribution of the crystallites. According to the theory of phase separation,¹⁴ the final polymer concentrations of concentrated and dilute phases are determined thermodynamically and are always the same irrespective of the total polymer concentration, so that the structure within the concentrated phase must be independent of the total polymer concentration. Taking into account that the crystallites are mainly produced in the concentrated phase and furthermore that the scattering intensity is governed by the strongest correlation between the nearest-neighbor crystallites, it is very natural that the correlation length is almost independent of the PVA concentration.

On the other hand, the correlation length ξ in the sol state ($C_p < 1.25$ g/dL) is rather small compared with that in the gel state, suggesting that the microgels formed in the sol state somewhat contract compared with the macroscopic gels. Below the critical gelation concentration where the infinite network is not produced even in the concentrated phase, the microgels are separately dispersed. Therefore, the crystallites in the microgels gather more closely than those in the infinite network in the macroscopic gels, leading to a slightly smaller correlation length. It is also noted in Figure 6 that the ξ of the gel ($C_p > 1.25$ g/dL) slightly increases with C_p . This fact may be also explained in the same way as for the smaller ξ of the sols. The fraction of the concentrated phase in the system increases with C_p , while the concentration within the concentrated phase is independent of C_p . As C_p decreases, the amount of the concentrated phase decreases so that it becomes difficult to make the infinite three-dimensional network of the concentrated phase, resulting in an increase of isolated clusters of the concentrated phase. These isolated clusters can be regarded as microgels, which give smaller ξ . Therefore, the average ξ slightly increases with C_p even in the gel state. The picture obtained here for the PVA gels can be improved by further studies using scattering techniques as well as other techniques.

In Figure 7, the correlation length ξ is plotted against the degree of polymerization P_n for the PVA concentration of $C_p = 5$ g/dL. The values of $\xi = 148$ and 160 Å for $P_n = 1640$ and 590, respectively, are almost the same, while $\xi = 208$ Å for $P_n = 186$ is fairly larger than the former values. As discussed above, it is considered that the correlation length ξ is determined by intercrystallite correlation, which is related to the distribution of crystallites in the concentrated phase. Almost the same values of ξ for $P_n = 1640$ and 590 indicate that the distributions of crystallites in the concentrated phase are similar for the both molecular weights, and the larger value for $P_n = 186$ may suggest that the average intercrystallite distance is larger than that for $P_n = 1640$ and 590. In other words, the number density of the crystallites for $P_n = 186$ is lower

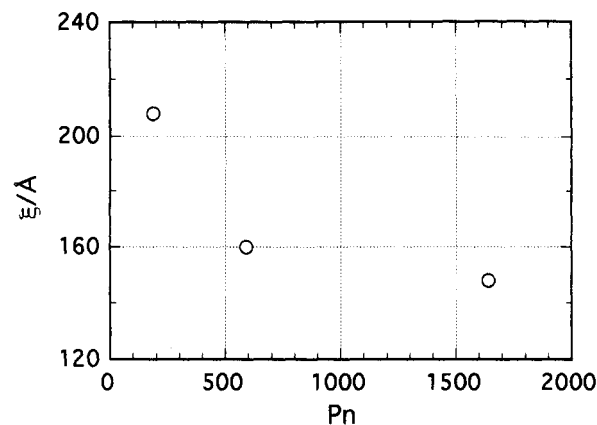


Figure 7. Correlation length ξ as a function of degree of polymerization P_n . The PVA concentration C_p is 5 g/dL.

than that for $P_n = 1640$ and 590. It is well-known that crystallization of polymer chains is hindered by entanglements, which is more effective for larger molecular weight. Therefore, it is considered that the crystallites for $P_n = 186$ may become larger than those for $P_n = 590$ and 1640, leading to a fewer number of crystallites for $P_n = 186$ than for $P_n = 590$ and 1640. This results in a larger average nearest-neighbor crystallite distance. It is noted that the correlation length ξ is not determined by the average size of PVA molecules such as radius of gyration. Radii of gyration are 131, 75, and 45 Å for $P_n = 1640$, 590, and 186, which were calculated under the assumption of a Gaussian chain using the persistence length 8 Å.¹⁴ For $P_n = 1640$, the value of the radius of gyration (131 Å) is rather close to that of the correlation length (168 Å). However, the molecular weight dependence of ξ is very different from that of the radius of gyration, confirming that the correlation length ξ is not determined by the average size of PVA molecules but by the correlation between the crystallites.

In order to see other aspects of the scattering curve, we calculated distance distribution function $P(r)$, which is defined by inverse Fourier-transformation of scattering intensity $I(Q)$,¹⁵

$$P(r) \sim (2/\pi) \int r Q I(Q) \sin(rQ) dQ \quad (3)$$

$$\sim 4\pi r^2 \gamma(r)$$

where $\gamma(r)$ is a pair correlation function. For calculation of eq 3, we have to extrapolate the observed scattering curves to both the lower and higher Q ranges. This was made by employing the functions of $I(0)/(1 + \xi^2 Q^2)$ and Q^{-4} for the lower and higher Q ranges, respectively. The calculated distance distribution functions $P(r)$ after normalizing by C_p are shown in Figure 8 for $P_n = 1640$ as a function of PVA concentration C_p . Two broad peaks or shoulders are observed at about 70 and 200 Å in $P(r)$ for all the PVA concentrations. The shapes of $P(r)$'s are also similar to one another for all the PVA concentrations except $C_p = 0.5$ and 1.0 g/dL, which are not macroscopically gels. For $C_p = 0.5$ and 1.0 g/dL, $P(r)$ in the r range larger than ca. 150 Å is rather small compared with the gel samples. This problem will be discussed later. Following the discussion on the small-angle scattering intensity $I(Q)$, the peaks or shoulders at about 70 and 200 Å may be assigned to the intra- and intercrystallite correlations, respectively. The position of the peak due to the intercrystallite correlation (~ 200 Å) is larger than the correlation length ξ evaluated from $I(Q)$ in the low Q range (see Figure 6). This is because the value of $P(r)$ at around $r = 200$ Å is mainly determined by $I(Q)$ at around $Q =$

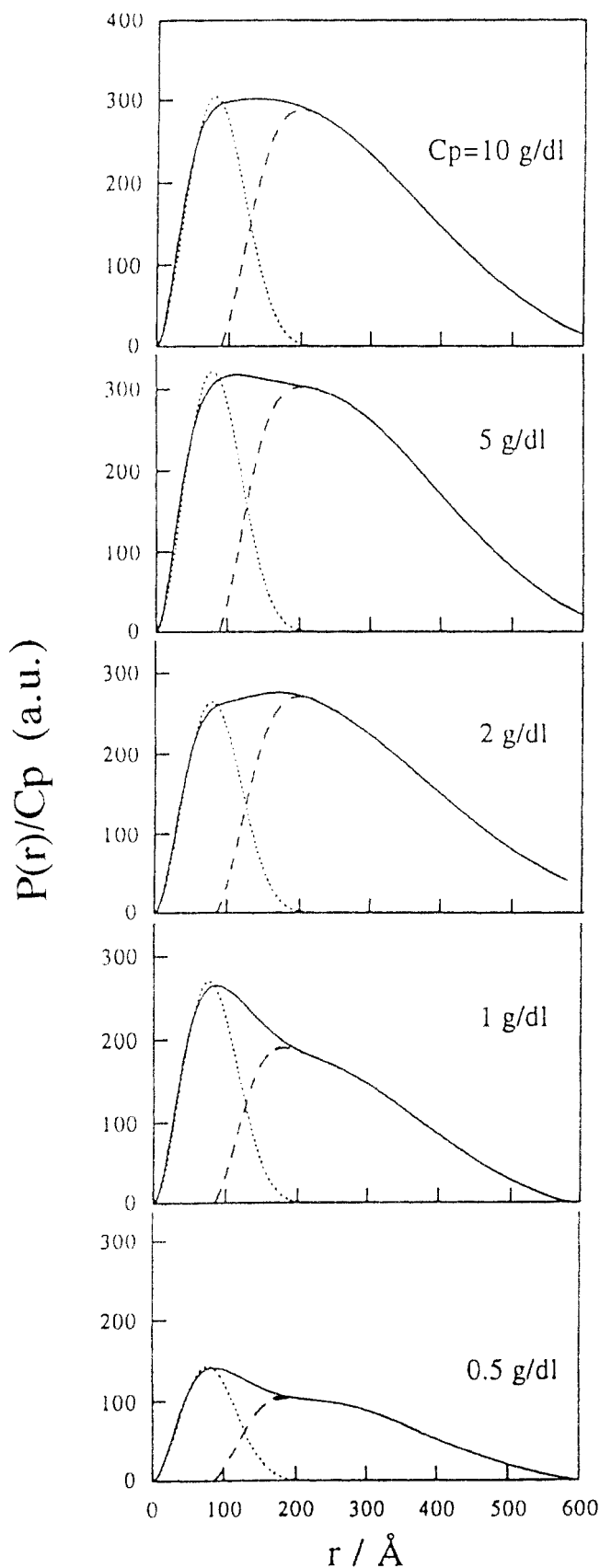


Figure 8. Distance distribution function $P(r)$ for PVA gels ($C_p = 10, 5$, and 2 g/dL) and sols ($C_p = 1$ and 0.5 g/dL) at 23 °C as a function of PVA concentration C_p . $P(r)$ is normalized by C_p . Dotted lines are the distance distribution function due to the intracrystallite correlation $P_{\text{intra}}(r)$, which was obtained by fitting a model function with the observed $P(r)$ in the small r range. The model function was calculated under the assumption that the shape of the crystallite is a sphere and the distribution of the sizes can be represented by a Gaussian. Dashed lines are the distance distribution function due to the intercrystallite correlation $P_{\text{inter}}(r)$, which was obtained by subtracting $P_{\text{intra}}(r)$ from the total $P(r)$.

Table 1. Radius of the Crystallite R and the Distribution of the Radius σ_c Evaluated by Fitting of $P(r)$

C_p /(g·dL ⁻¹)	R /Å	σ_c /Å	state
0.5	73.4	15.3	sol
1.0	71.9	15.2	sol
2.0	73.4	15.4	gel
5.0	74.5	14.9	gel
10.0	73.7	16.4	gel

$2\pi/200$ but also slightly affected by $I(Q)$ in the high Q range ($Q > 0.05$ Å⁻¹), where $I(Q)$ is not described by the OZ formula but by Q^{-4} .

The distance distribution function $P(r)$ is more useful in the understanding of the distribution of the crystallites intuitively than the scattering intensity $I(Q)$. However, $P(r)$ includes both contributions of the intra- and intercrystallite correlations. In order to separate two contributions, we fitted the observed $P(r)$ in the small r range with a model function for intracrystallite correlation. This model function was calculated under the assumption that the shape of the crystallites is a sphere and the size (radius) distribution of the crystallites can be represented by a Gaussian. The dotted lines in Figure 8 show the results of the fit, which corresponds to the distance distribution function due to intracrystallite correlation $P_{\text{intra}}(r)$. The sizes (radii) and the size distributions (root of the dispersion σ_c) are listed in Table 1. The radii evaluated by the fitting are about 70 Å for all the PVA concentrations. The dashed lines in Figure 8 show the intercrystallite correlation $P_{\text{inter}}(r)$, which was obtained by subtracting $P_{\text{intra}}(r)$ from the total $P(r)$. Roughly speaking, $P_{\text{inter}}(r) dr$ is proportional to the number of pairs of crystallites in the r range of $r \sim r + dr$. The peak position may correspond to the average distance between the nearest-neighbor crystallites, and the long tail of $P_{\text{inter}}(r)$ in the larger r range may also correspond to the second- and third-neighbor correlations of crystallites.

$P_{\text{inter}}(r)$ is almost independent of C_p in the gel region ($C_p > 1.25$ g/dL at 23 °C) because the crystallites are mainly produced in the concentrated phase after liquid-liquid phase separation and the concentration in that phase is independent of C_p as discussed above. On the other hand, $P_{\text{inter}}(r)$ for the sol state ($C_p = 0.5$ and 1.0 g/dL) is different from that for the gel state; e.g., the peak positions of $P_{\text{inter}}(r)$ are about 170 Å which are rather small compared with the gels (~ 200 Å), and the intensities of $P_{\text{inter}}(r)$ for the sols are smaller than those for the gels. As discussed above, even in the sol states the PVA solutions can be regarded as microgels. The crystallites can gather closer to each other in the microgels because the microgels are isolated from each other, leading to the shorter intercrystallite distance. This picture well explains the fact that the peak position of $P_{\text{inter}}(r)$ for the sol ($C_p = 0.5$ and 1.0 g/dL) appears at the smaller value (~ 170 Å). Furthermore, the small intensity of $P_{\text{inter}}(r)$ can be explained as follows. The intensity of $P_{\text{inter}}(r)$ is roughly proportional to the number of the nearest neighboring crystallites around a marked crystallite. When the marked crystallite is on a surface of the microgel domains (the concentrated phase), this number is less than when it is inside the domains. The surface-to-volume ratio in the concentrated phase for the microgel state is certainly larger than that for the gel state because of the small average size of the microgels, resulting in the smaller value of $P_{\text{inter}}(r)$. This is the reason why $P_{\text{inter}}(r)$'s for $C_p = 0.5$ and 1.0 g/dL are smaller than those for $C_p = 2, 5$, and 10 g/dL.

Conclusions

The PVA gels in a mixture of dimethyl sulfoxide (DMSO) and water were studied by wide- and small-angle

neutron scattering techniques. One of the most important findings here is that the cross-linking points of the gels are crystallites. This fact gives us a basis for interpretation of the results of the SANS measurements. We further found the following results. The surface boundaries of the crystallites are rather clear, the average size (radius) of the crystallites is about 70 Å, the average distance between the nearest-neighbor crystallites is about 150–200 Å, and there is microgel structure even in the sol state. It was also found that the distance distribution function $P(r)$ is very useful to intuitively understand the distribution of the crystallites.

In the Q range accessible by the present SANS measurements, it was impossible to detect the phase-separated structure directly, but it is emphasized that the present results do not contradict the idea that the liquid–liquid phase separation takes place before gelation. In fact, some of the present results have been well explained by the idea of the phase separation. At the present stage, however, the structure due to the phase separation is not well understood, which is one of the most challenging problems in the future. Furthermore, kinetics of the gel formation must be studied in order to clarify the relation between the phase separation and the gelation. These studies are now in progress.

References and Notes

- (1) Labudzinska, A.; Ziabicki, A. *Kolloid Z. Z. Polym.* **1971**, *243*, 21.
- (2) Hyon, S.-H.; Cha, W.-I.; Ikada, Y. *Polym. Bull.* **1989**, *22*, 119.
- (3) Ohkura, M.; Kanaya, T.; Kaji, K. *Polymer* **1992**, *33*, 3686.
- (4) Ohkura, M.; Kanaya, T.; Kaji, K. *Polymer* **1992**, *33*, 5044.
- (5) Pines, E.; Prins, W. *Macromolecules* **1978**, *6*, 888.
- (6) Komatsu, M.; Inoue, T.; Miyasaka, K. *J. Polym. Sci., Polym. Phys. Ed.* **1986**, *24*, 303.
- (7) Wu, W.; Shibayama, M.; Kurokawa, H.; Coyne, L. D.; Nomura, S.; Stein, R. *Macromolecules* **1990**, *23*, 2246.
- (8) Wu, W.; Kurokawa, H.; Roy, S.; Stein, R. *Macromolecules* **1991**, *24*, 4328.
- (9) Shibayama, M.; Kurokawa, H.; Nomura, S.; Muthukumar, M.; Stein, R.; Roy, S. *Polymer* **1992**, *33*, 2883.
- (10) Ishikawa, Y.; Furusaka, M.; Niimura, N.; Arai, M.; Hasegawa, K. *J. Appl. Crystallogr.* **1986**, *19*, 229.
- (11) Misawa, M.; Fukunaga, T.; Yamaguchi, T.; Watanabe, N. *Proceedings of International Conference on Advanced Neutron Source*; Atchison, F., Fischer, W., Eds.; Villigen, 1986, Vol. IX.
- (12) Bunn, C. W. *Nature* **1948**, *161*, 929.
- (13) Flory, P. J. *Principles of Polymer Chemistry*; Cornell University Press: Ithaca, NY, 1953.
- (14) *Polymer Handbook*, 3rd ed. Brandrup, J., Immergut, E. H., Eds.; Wiley-Interscience: New York, 1989; Vol. VII.
- (15) Kaji, K.; Urakawa, H.; Kanaya, T.; Kitamaru, R. *Macromolecules* **1984**, *17*, 1835.